

ORIGINAL ARTICLE

UDC 577.322.4

doi: 10.26907/2542-064X.2022.2.185-195

ATOMISTIC SIMULATIONS OF PAP248-286 PEPTIDE OLIGOMERIZATION

A.O. Nikitina, A.R. Yulmetov, A.M. Kusova, V.V. Klochkov, D.S. Blokhin

Kazan Federal University, Kazan, 420008 Russia

Abstract

Amyloid fibrils, dubbed SEVI (semen-derived enhancer of virus infection), contribute to the spread of HIV infection. The main components of SEVI are the fragments of prostatic acid phosphatase (PAP): PAP248-286 and PAP85-120. SEVI captures the viral particles and further stimulates their attachment to the target cells, thereby boosting viral fusion and infection. To study the oligomers of SEVI-forming peptides, we used molecular modeling, which is a powerful tool that has been applied in a great variety of studies on SEVI, and an advanced accelerated sampling method of metadynamics. Based on the obtained molecular dynamics data, it was shown that PAP248-286 has a horseshoe shape with bends in the regions of amino acid residues A274 and N269 in the dimeric state. It was suggested that the horseshoe shape might lead in the fibrillation process to the steric zipper model formation, which is typical of amyloids. It was confirmed that the process of fibril formation of PAP248-286 starts with a pairwise parallel arrangement of the peptide helical regions.

Keywords: HIV, prostatic acid phosphatase, SEVI, molecular dynamics, metadynamics

Introduction

Amyloid fibrils are ordered aggregates of soluble proteins and peptides that are related to more than 20 human disorders, including Alzheimer's, Parkinson's, and Huntington's diseases, as well as HIV infection [1–4]. The pathological manifestation of an amyloid condition results from the association of certain proteins, which is the main driving force for the fibril structure formation [5–7]. The effectiveness of treatment depends, in many ways, on our better understanding of the physicochemical parameters of amyloid fibrils. Several comprehensive studies of self-assembly mechanisms of functional and pathogenic polypeptides have been performed in the last three decades [8–11]. Many experimental studies of structural rearrangements in amyloidogenic polypeptides have been hampered by the presence of intrinsically disordered fragments with both high flexibility and ability to bind with a large number of partner proteins [12, 13].

This article focuses on the initial stage of fibril formation of the C-terminal region of prostatic acid phosphatase (PAP), which is termed as a semen-derived enhancer of viral infection (SEVI). The peptide PAP248–286 is a proteolytic cleavage product of PAP, a protein found in abundant quantities in semen. In [11, 15], it was shown that soluble PAP248-286 had no effect on HIV infectivity, whereas SEVI augmented HIV infection by $\sim 10^5$ fold. These fibrils normally possess a high net positive charge

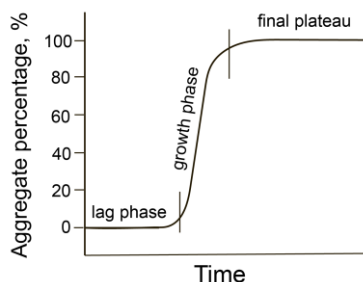


Fig. 1. Percentage of proteins included in aggregation as a function of time

at neutral pH [16–18] and form a cationic bridge precipitating the virus on the cell surface and reducing electrostatic repulsion between the negatively charged surfaces of the virus and the host cell [17–20]. SEVI binds to both HIV virions and target cells, thereby increasing viral attachment, fusion, and infection. Due to its stable structure and high concentration in semen, SEVI is an attractive drug target for preventing HIV infection [21–23].

The secondary structure of PAP248-286 is highly disordered in solution, whereas amyloidogenic peptides can undergo reversible structural transformations into more ordered states, such as helices and β -chains upon amyloid fibrils formation [14, 15]. The kinetics of fibril formation process has been widely analyzed and exhibits the following three characteristic stages on a macroscopic level: a lag phase, a growth phase, and a final plateau regime (Fig. 1) [24, 25]. The lag phase is of particular interest because it provides important information about the factors regulating the fibrillation process. The formation of small oligomers precedes ordered nucleus formation and subsequent rapid fibril growth. A major practical and research problem is to identify the molecular mechanisms that underlie the lag phase in fibril formation [26].

In this study, we have carried out a systematic molecular dynamic (MD) simulation to analyze PAP248-286 oligomerization during the lag phase. The MD approach is a suitable tool to observe the molecular processes that are not experimentally detectable [27]. However, its applicability is limited by the computation time. Accelerated sampling methods, such as metadynamics [28, 29] and thermodynamics [30] modeling and umbrella sampling [31], have been proposed to reduce this limitation and to monitor the polypeptide oligomerization. Metadynamics procedures show definite promise for restoring the free-energy surface and for accelerating rare events in systems described by Hamiltonians (H) on the classical or quantum levels, they introduce a bias potential (U_{bias}) that lowers energy barriers between conformational states, thus accelerating the system passage of the conformational space by avoiding the already passed states:

$$H = T + U + U_{\text{bias}},$$

where U is the potential energy of a system, T is its kinetics energy, and U_{bias} is the function of the reaction coordinates known as collective variables (CV).

The distance between the centers of mass R and the number of specific monomer-monomer contacts N_{CV} measured using the Plumed plugin [32] are deemed as CV.

MD represents a suitable approach for the design of point mutations that affect the aggregation process of the PAP248-286 peptide. Modeling of the PAP248-286

peptide oligomers can help to identify amyloidogenic regions in peptide. In this work, we performed a systematic MD analysis of all atoms of two, three, four, six, and seven PAP248-286 molecules using the metadynamics method.

1. Methods

Initial conformations of PAP248-286 peptide were obtained from the monomeric nuclear magnetic resonance structure (PDB ID 2L3H). All of the simulations were done with the help of the GROMACS 2020 MD code [33] and the PLUMED plugin [32]. The Charmm36 [34] and TIP3P [35] models were used for protein and water molecules, respectively. To create conditions close to physiological, Cl^- and Na^+ ions were added to the system (150 mM). The solvent was equilibrated around the protein in two phases: (1) NVT (constant number of particles, volume, and temperature) for 100 ps to stabilize the temperature (300 K) by applying Berendsen thermostat algorithm; (2) system equilibration for pressure (1 bar) in the NPT step (constant number of particles, pressure, and temperature) for 100 ps using Nose-Hoover thermostat. After the system equilibration, the final run was performed for 100 ns for each system using same pressure, temperature, and integrator. To accelerate sampling, the metadynamics method was used in all steps of the oligomerization process modeling. Metadynamics modeling was implemented in the GROMACS software package with the PLUMED plugin to construct the free-energy profiles of oligomers. The bias potential U_{bias} , collective variables (CV), and additional forces were calculated. The metadynamics bias was applied to both configurational CVs – the distance between the centers of mass of the monomers (R) and the number of specific monomer-monomer contacts (N_{CV}). For the metadynamics setup, Gaussian functions of height $w = 0.25$ kJ/mol were added every 2 ps, and U_{bias} exchanges were attempted every 20 ps. Then, based on the total values of energy and forces, the atomic coordinates were updated using the GROMACS software package for the next step – molecular dynamics modeling. The duration of trajectories was 100 ns; the metadynamics frames were saved every 10 ps. The UCSF Chimera program was used for the visualization of structures [36].

2. Results and Discussion

Our results concern the amyloidogenic peptide PAP248-286 oligomers (dimer, trimer, tetramer, hexamer, and heptamer). Let us first consider the process of peptide dimerization modeling. The monomer structure of PAP248-286 peptide (PDB database, PDB ID 2L3H) was equilibrated using molecular modeling. Then, a PDB file was created with two PAP248-286 molecules for subsequent MD simulations with metadynamics. The bias potential U_{bias} has been included in calculation by metadynamics. U_{bias} was regarded as a function of the collective variables (R , N_{CV}). N_{CV} was defined by the distance between molecules less than 0.3 nm calculated using the PLUMED plugin.

With the help of molecular modeling, a map of free energy ΔF as a function of the CV R and N_{CV} was obtained (Fig. 2). The map exhibits a wide global minimum in the region of $R = 1.9$ nm. This is also illustrated in the plot of free energy ΔF vs R (Fig. 3). For verification of the stability of the dimer structure, the minimum free-energy

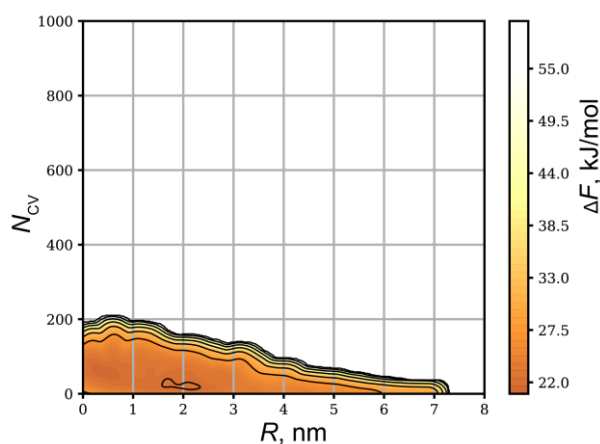


Fig. 2. Free-energy surface of the PAP248-286 dimerization process as a function of R and N_{CV}

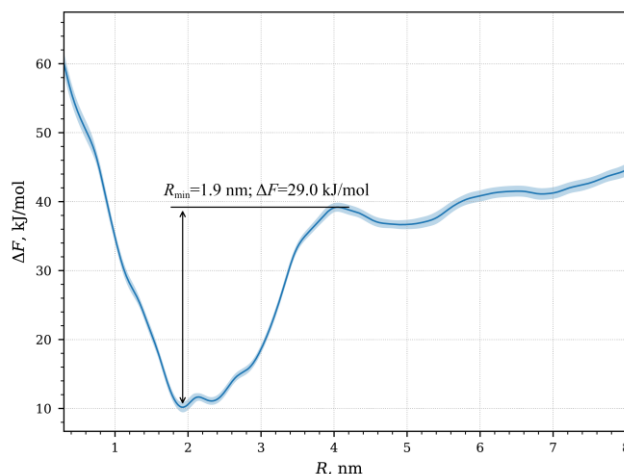


Fig. 3. The plot of the free energy ΔF vs R for the process of PAP248-286 dimerization

simulations were carried out without the use of metadynamics. For MD simulations, the backbone chain RMSD (Fig. 4, *a*) and the radius of gyration (Fig. 4, *b*) of the dimer were obtained by the analysis of the coordinate trajectory. The changes in RMSD and the gyration radius values indicate the stability of the PAP248-286 dimer during the simulation time. In Fig. 5, the final dimer structure with the minimum of free energy is shown.

Higher-order PAP248-286 oligomers were modeled in a similar manner. The polypeptide trimer was simulated by adding a monomer to the dimer in a cubic cell using the algorithm described above. The tetramer was simulated as two dimers initially located at opposite ends of the cubic cell. The hexamer was composed as a tetramer and a dimer initially located at opposite ends of the cell. The heptamer was obtained by adding a monomer polypeptide to the previous one. The free energy maps and the final structures of PAP248-286 oligomers corresponding to the global free energy minimum are shown in Figs. 6 and 7, respectively.

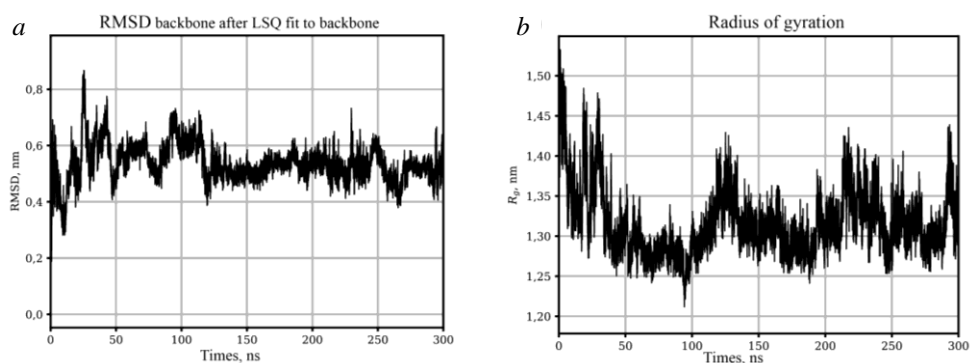


Fig. 4. Backbone chain RMSD (a) and radius of gyration (b) of the PAP248-286 dimer

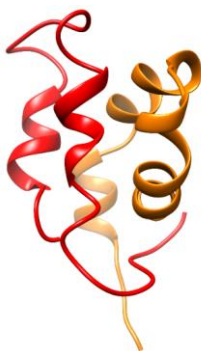


Fig. 5. Structure of the PAP248-286 dimer corresponding to the global minimum of free-energy surface

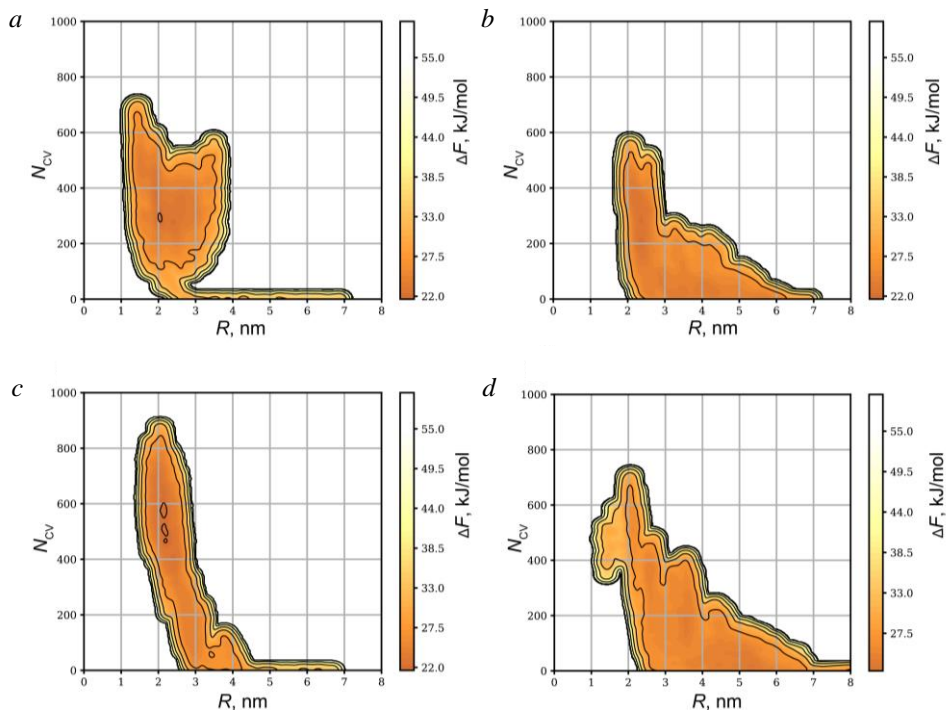


Fig. 6. Free-energy surface of PAP248-286: a) trimer, b) tetramer, c) hexamer, and d) heptamer

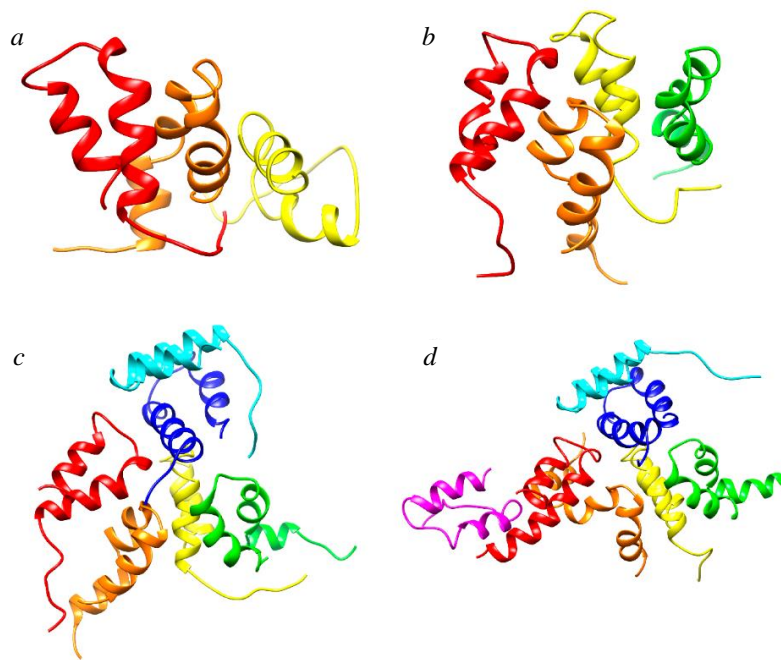


Fig. 7. Structure of PAP248-286: *a*) trimer, *b*) tetramer, *c*) hexamer, and *d*) heptamer. The structures correspond to the global minimum of free-energy surfaces. Key: molecule 1 – red, molecule 2 – orange, molecule 3 – yellow, molecule 4 – green, molecule 5 – cyan, molecule 6 – blue, molecule 7 – magenta

The spatial structure of the monomer peptide PAP248-286 (PDB ID: 2L3H) has two ordered helical fragments: V262-L268 and K281-I284. Through molecular modeling, we showed that PAP248-286 molecules have a horseshoe shape with bends in the regions of amino acid residues A274 and N269 in the dimeric state. PAP248-286 dimers contain α -helices V262-H270 and I277-L283. The positions of the helical regions (PDB ID 2L3H) in the polypeptide monomer and dimer coincide, but their length and proximity are higher for the dimer state than for the monomer state. Similar structural changes were observed for higher-order oligomers of PAP248-286 (Fig. 7). Thus, the increase in the length of the helical regions and their parallel arrangement are consistent with the mechanism of amyloid formation proposed by G. Liu et al. [37]. We can suggest that the horseshoe shape of the backbone chain may cause further transformation of α -helices into β -sheets and the formation of a steric zipper model typical of amyloids [38].

In Fig. 7, you can see that for all PAP248-286 oligomers there is a parallel arrangement of the helical regions for two molecules, as observed for the dimer form. For all oligomer forms of PAP248-286, a pairwise parallel arrangement of helical regions was observed, which supports the assumption about the second stage in the lag phase of fibril formation [37]. There is a deviation from the parallel arrangement of the unpaired molecule for the odd order of the PAP248-286 oligomer. The third molecule does not have a parallel helical region to ones of the dimeric pair in the polypeptide trimer (Fig. 7, *b*). The helical region of the seventh molecule in the heptamer aligns in parallel to the helical regions of the first molecule breaking the parallelism within

the pair of molecules 1 and 2 (Fig. 7, *d*). Based on the data obtained, it can be concluded that the beginning of the PAP248-286 fibril formation process is characterized by a pairwise parallel arrangement of the helical regions of the polypeptide molecules that occur in all oligomers.

Conclusions

In this article, we shed light on some problematic issues concerning oligomers of the amyloidogenic peptide PAP248-286 obtained by MD modeling based on the metadynamics approach. The amyloidogenic peptide PAP248-286 oligomers (dimer, trimer, tetramer, hexamer, and heptamer) structures were investigated. It was shown that the structures of polypeptide oligomers under consideration correspond to the global energy minimum on the free energy map. The backbone chain of PAP248-286 oligomer contains bends in the regions of amino acid residues A274 and N269. This backbone chain has the horseshoe shape that could favor the steric zipper amyloid formation model at the next stages of fibrillation. The increase in the length of the helical regions and their parallel arrangement caused by the oligomerization process was consistent with the mechanism of amyloid formation proposed by G. Liu et al. [37]. The data obtained can be used to develop an approach to point mutations design with reference to the PAP248-286 fibrillation process. Point mutations in the amino acid residues A274 and N269 (for example, proline insertions) could hinder the backbone bending and prevent the formation of steric zipper. This may create difficulties during the process of PAP248-286 fibrillation.

Acknowledgments. This work is supported by the Russian Science Foundation (project no. 20-73-10034). D.S. Blokhin acknowledges the funding from the RF Presidential Council for the State Support of Young Russian Scientists (Candidates of Sciences), project MK-938.2020.4.

References

1. Chiti F., Dobson C.M. Protein misfolding, functional amyloid, and human disease. *Annu. Rev. Biochem.*, 2006, vol. 75, no. 1, pp. 333–366. doi: 10.1146/annurev.biochem.75.101304.123901.
2. Buchanan L.E., Dunkelberger E.B., Tran H.Q., Cheng P.-N., Chiu Ch.-Ch., Cao P., Raleigh D.P., de Pablo J.J., Nowick J.S., Zanni M.T. Mechanism of IAPP amyloid fibril formation involves an intermediate with a transient β -sheet. *Proc. Natl. Acad. Sci. U. S. A.*, 2013, vol. 110, no. 48, pp. 19285–19290. doi: 10.1073/pnas.1314481110.
3. Münch J., Sauer mann U., Yolamanova M., Raue K., Stahl-Hennig Ch., Kirchhoff F. Effect of semen and seminal amyloid on vaginal transmission of simian immunodeficiency virus. *Retrovirology*, 2013, vol. 10, art. 148, pp. 1–9. doi: 10.1186/1742-4690-10-148.
4. Sievers S.A., Karanicolas J., Chang H.W., Zhao A., Jiang L., Zirafi O., Stevens J.T., Münch J., Baker D., Eisenberg D. Structure-based design of non-natural amino-acid inhibitors of amyloid fibril formation. *Nature*, 2011, vol. 475, no. 7354, pp. 96–100. doi: 10.1038/nature10154.
5. Dobson C.M. The structural basis of protein folding and its links with human disease. *Philos. Trans. R. Soc., B*, 2001, vol. 356, no. 1406, pp. 133–145. doi: 10.1098/rstb.2000.0758.
6. Kelly J.W. Towards an understanding of amyloidogenesis. *Nat. Struct. Biol.*, 2002, vol. 9, no. 5, pp. 323–325. doi: 10.1038/nsb0502-323.

7. Zerovnik E. Amyloid-fibril formation. Proposed mechanisms and relevance to conformational disease. *Eur. J. Biochem.*, 2002, vol. 269, no. 14, pp. 3362–3371. doi: 10.1046/j.1432-1033.2002.03024.x.
8. Habibi N., Kamaly N., Memic A., Shafiee H. Self-assembled peptide-based nanostructures: Smart nanomaterials toward targeted drug delivery. *Nano Today*, 2016, vol. 11, no. 1, pp. 41–60. doi: 10.1016/j.nantod.2016.02.004.
9. Ilie I.M., Cafilisch A. Simulation studies of amyloidogenic polypeptides and their aggregates. *Chem. Rev.*, 2019, vol. 119, no. 12, pp. 6956–6993. doi: 10.1021/acs.chemrev.8b00731.
10. Lotan T., Ori N., Fluhr R. Pathogenesis-related proteins are developmentally regulated in tobacco flowers. *The Plant Cell*, 1989, vol. 1, no. 9, pp. 881–887. doi: 10.1105/tpc.1.9.881.
11. Münch J., Rücker E., Ständker L., Adermann K., Goffinet Ch., Schindler M., Wildum S., Chinnadurai R., Rajan D., Specht A., Giménez-Gallego G., Sánchez P.C., Fowler D.M., Koulov A., Kelly J.W., Mothes W., Grivel J.-Ch., Margolis L., Keppler O.T., Forssmann W.-G., Kirchhoff F. Semen-derived amyloid fibrils drastically enhance HIV infection. *Cell*, 2007, vol. 131, no. 6, pp. 1059–1071. doi: 10.1016/j.cell.2007.10.014.
12. Uversky V.N., Oldfield C.J., Dunker A.K. Intrinsically disordered proteins in human diseases: Introducing the D² concept. *Annu. Rev. Biophys.*, 2008, vol. 37, pp. 215–246. doi: 10.1146/annurev.biophys.37.032807.125924.
13. Uversky V.N. Intrinsically disordered proteins from A to Z. *Int. J. Biochem. Cell Biol.*, 2011, vol. 43, no. 8, pp. 1090–1103. doi: 10.1016/j.biocel.2011.04.001.
14. Uversky V.N. Targeting intrinsically disordered proteins in neurodegenerative and protein dysfunction diseases: Another illustration of the D² concept. *Expert Rev. Proteomics*, 2010, vol. 7, no. 4, pp. 543–564. doi: 10.1586/epr.10.36.
15. Castellano L.M., Shorter J. The surprising role of amyloid fibrils in HIV infection. *Biology*, 2012, vol. 1, no. 1, pp. 58–80. doi: 10.3390/biology1010058.
16. Avni A., Swasthi H.M., Majumdar A., Mukhopadhyay S. Intrinsically disordered proteins in the formation of functional amyloids from bacteria to humans. *Prog. Mol. Biol. Transl. Sci.*, 2019, vol. 166, pp. 109–143. doi: 10.1016/bs.pmbts.2019.05.005.
17. Roan N.R., Müller J.A., Liu H., Chu S., Arnold F., Stürzel Ch.M., Walther P., Dong M., Witkowska H.E., Kirchhoff F., Münch J., Greene W.C. Peptides released by physiological cleavage of semen coagulum proteins form amyloids that enhance HIV infection. *Cell Host Microbe*, 2011, vol. 10, no. 6, pp. 541–550. doi: 10.1016/j.chom.2011.10.010.
18. Roan N.R., Münch J., Arhel N., Mothes W., Neidleman J., Kobayashi A., Smith-McCune K., Kirchhoff F., Greene W.C. The cationic properties of SEVI underlie its ability to enhance human immunodeficiency virus infection. *J Virol.*, 2009, vol. 83, no. 1, pp. 73–80. doi: 10.1128/jvi.01366-08.
19. Arcasoy S.M., Latoche J.D., Gondor M., Pitt B.R., Pilewski J.M. Polycations increase the efficiency of adenovirus-mediated gene transfer to epithelial and endothelial cells in vitro. *Gene Ther.*, 1997, vol. 4, no. 1, pp. 32–38. doi: 10.1038/sj.gt.3300349.
20. Davis H.E., Morgan J.R., Yarmush M.L. Polybrene increases retrovirus gene transfer efficiency by enhancing receptor-independent virus adsorption on target cell membranes. *Biophys. Chem.*, 2002, vol. 97, nos. 2–3, pp. 159–172. doi: 10.1016/s0301-4622(02)00057-1.
21. Duan J.-M., Qiu J.-Y., Tan S.-Y., Liu S.-W., Li L. Semen-derived enhancer of viral infection – a key factor in sexual transmission of HIV. *Bing Du Xue Bao*, 2012, vol. 28, pp. 84–88.
22. Ren R., Yin S., Lai B., Ma L., Wen J., Zhang X., Lai F., Liu Sh., Li L. Myricetin antagonizes semen-derived enhancer of viral infection (SEVI) formation and influences its infection-enhancing activity. *Retrovirology*, 2018, vol. 15, art. 49, pp. 1–24. doi: 10.1186/s12977-018-0432-3.

23. Zhang X., Chen J., Yu F., Wang Ch., Ren R., Wang Q., Tan S., Jiang Sh., Liu Sh., Li L. 3-hydroxyphthalic anhydride-modified rabbit anti-PAP IgG as a potential bifunctional HIV-1 entry inhibitor. *Front. Microbiol.*, 2018, vol. 9, art. 1330, pp. 1–18. doi: 10.3389/fmicb.2018.01330.
24. Cohen S.I.A., Vendruscolo M., Dobson C.M., Knowles T.P.J. From macroscopic measurements to microscopic mechanisms of protein aggregation. *J. Mol. Biol.*, 2012, vol. 421, nos. 2–3, pp. 160–171. doi: 10.1016/j.jmb.2012.02.031.
25. Shoffner S.K., Schnell S. Estimation of the lag time in a subsequent monomer addition model for fibril elongation. *Phys. Chem. Chem. Phys.*, 2016, vol. 18, no. 31, pp. 21259–21268. doi: 10.1039/C5CP07845H.
26. Arosio P., Knowles T.P.J., Linse S. On the lag phase in amyloid fibril formation. *Phys. Chem. Chem. Phys.*, 2015, vol. 17, no. 12, pp. 7606–7618. doi: 10.1039/c4cp05563b.
27. Piñeiro Á., Villa A., Vagt T., Kokscho B., Mark A.E. A molecular dynamics study of the formation, stability, and oligomerization state of two designed coiled coils: Possibilities and limitations. *Biophys. J.*, 2005, vol. 89, no. 6, pp. 3701–3713. doi: 10.1529/biophysj.104.055590.
28. Laio A., Parrinello M. Escaping free-energy minima. *Proc. Natl. Acad. Sci. U. S. A.*, 2002, vol. 99, no. 20, pp. 12562–12566. doi: 10.1073/pnas.202427399.
29. Sutto L., Marsili S., Gervasio F.L. New advances in metadynamics. *WIREs Comput. Mol. Sci.*, 2012, vol. 2, no. 5, pp. 771–779. doi: 10.1002/wcms.1103.
30. Ruiz-Montero M.J., Frenkel D., Brey J.J. Efficient schemes to compute diffusive barrier crossing rates. *Mol. Phys.*, 1997, vol. 90, no. 6, pp. 925–942. doi: 10.1080/002689797171922.
31. Torrie G.M., Valleau J.P. Nonphysical sampling distributions in Monte Carlo free-energy estimation: Umbrella sampling. *J. Comput. Phys.*, 1977, vol. 23, no. 2, pp. 187–199. doi: 10.1016/0021-9991(77)90121-8.
32. Tribello G.A., Bonomi M., Branduardi D., Camilloni C., Bussi G. PLUMED 2: New feathers for an old bird. *Comput. Phys. Commun.*, 2014, vol. 185, no. 2, pp. 604–613. doi: 10.1016/j.cpc.2013.09.018.
33. Pronk S., Páll S., Schulz R., Larsson P., Bjelkmar P., Apostolov R., Shirts M.R., Smith J.C., Kasson P.M., van der Spoel D., Hess B., Lindahlet E. GROMACS 4.5: A high-throughput and highly parallel open source molecular simulation toolkit. *Bioinformatics*, 2013, vol. 29, no. 7, pp. 845–854. doi: 10.1093/bioinformatics/btt055.
34. Huang J., MacKerell A.D., Jr. CHARMM36 all-atom additive protein force field: Validation based on comparison to NMR data. *J. Comput. Chem.*, 2013, vol. 34, no. 25, pp. 2135–2145. doi: 10.1002/jcc.23354.
35. Jorgensen W.L., Chandrasekhar J., Madura J.D., Impey R.W., Klein M.L. Comparison of simple potential functions for simulating liquid water. *J. Chem. Phys.*, 1983, vol. 79, no. 2, pp. 926–935. doi: 10.1063/1.445869.
36. Pettersen E.F., Goddard T.D., Huang C.C., Couch G.S., Greenblatt D.M., Meng E.C., Ferrin T.E. UCSF Chimera – a visualization system for exploratory research and analysis. *J. Comput. Chem.*, 2004, vol. 25, no. 13, pp. 1605–1612. doi: 10.1002/jcc.20084.
37. Liu G., Prabhakar A., Aucoin D., Simon M., Sparks S., Robbins K.J., Sheen A., Petty S.A., Lazo N.D. Mechanistic studies of peptide self-assembly: Transient α -helices to stable β -sheets. *J. Am. Chem. Soc.*, 2010, vol. 132, no. 51, pp. 18223–18232. doi: 10.1021/ja1069882.
38. Goldschmidt L., Teng P.K., Riek R., Eisenberg D. Identifying the amyloids, proteins capable of forming amyloid-like fibrils. *Proc. Natl. Acad. Sci. U. S. A.*, 2013, vol. 107, no. 8, pp. 3487–3492. doi: 10.1073/pnas.0915166107.

Received
March 11, 2022

Nikitina Anna Olegovna, Student, Institute of Physics

Kazan Federal University
ul. Kremlevskaya, 18, Kazan, 420008 Russia
E-mail: annanikitina199737@gmail.com

Yulmetov Aydar Rafailevich, PhD in Physics and Mathematics, Associate Professor, Institute of Physics

Kazan Federal University
ul. Kremlevskaya, 18, Kazan, 420008 Russia
E-mail: ajulmeto@gmail.com

Kusova Aleksandra Mikhailovna, Junior Research Fellow, Institute of Physics

Kazan Federal University
ul. Kremlevskaya, 18, Kazan, 420008 Russia
E-mail: alexakusova@mail.ru

Klochkov Vladimir Vasilyevich, Doctor of Chemistry, Professor, Institute of Geology and Petroleum Technologies

Kazan Federal University
ul. Kremlevskaya, 18, Kazan, 420008 Russia
E-mail: vklochko@kpfu.ru

Blokhin Dmitriy Sergeevich, PhD in Physics and Mathematics, Associate Professor, Institute of Physics

Kazan Federal University
ul. Kremlevskaya, 18, Kazan, 420008 Russia
E-mail: dblohin@kpfu.ru

ОРИГИНАЛЬНАЯ СТАТЬЯ

УДК 577.322.4

doi: 10.26907/2542-064X.2022.2.185-195

**Атомистическое моделирование
олигомеризации пептида PAP248-286**

*А.О. Никитина, А.Р. Юльметов, А.М. Кусова, В.В. Клочков, Д.С. Блохин
Казанский (Приволжский) федеральный университет, г. Казань, 420008, Россия*

Аннотация

Амилоидные фибриллы, в состав которых входят фрагменты PAP248-286 и PAP85-120 простатической кислой фосфатазы (PAP), известны как SEVI (semen-derived enhancer of virus infection – усилители вирусной инфекции, полученные из семенной жидкости). Их присутствие связывают с повышенным риском инфицирования ВИЧ: захватывая вирионы, фибриллы SEVI помогают вирусу прикрепляться к клеткам-мишеням и таким образом многократно увеличивают его патогенность. Настоящее исследование посвящено изучению особенностей олигомеров SEVI-образующих пептидов путем построения их молекулярных моделей, доказавших свою эффективность в изучении SEVI, а также с использованием такого метода ускоренной выборки как метадинамика. На основе полученных данных молекулярной динамики было показано, что в димерном состоянии пептид PAP248-286 имеет подковообразную форму с изгибами в аминокислотных остатках A274 и N269, что на стадии образования фибриллярной структуры может способствовать реализации модели «стерической застёжки-молнии», свойственной амилоидам. Установлено, что фибриллы пептида образуются, когда его спиральные области становятся параллельны друг другу.

Ключевые слова: ВИЧ, простатическая кислая фосфатаза, SEVI, молекулярная динамика, метадинамика

Благодарности. Работа выполнена при поддержке Российского научного фонда (проект № 20-73-10034). Исследования Д.С. Блохина проводились в рамках гранта Президента РФ по государственной поддержке молодых российских ученых – кандидатов наук (проект № МК-938.2020.4).

Поступила в редакцию
11.03.2022

Никитина Анна Олеговна, студент Института физики

Казанский (Приволжский) федеральный университет
ул. Кремлевская, д. 18, г. Казань, 420008, Россия
E-mail: annanikitina199737@gmail.com

Юльметов Айдар Рафаилович, кандидат физико-математических наук, доцент Института физики

Казанский (Приволжский) федеральный университет
ул. Кремлевская, д. 18, г. Казань, 420008, Россия
E-mail: ajulmeto@gmail.com

Кусова Александра Михайловна, младший научный сотрудник Института физики

Казанский (Приволжский) федеральный университет
ул. Кремлевская, д. 18, г. Казань, 420008, Россия
E-mail: alexakusova@mail.ru

Клочков Владимир Васильевич, доктор химических наук, профессор Института геологии и нефтегазовых технологий

Казанский (Приволжский) федеральный университет
ул. Кремлевская, д. 18, г. Казань, 420008, Россия
E-mail: vklochko@kpfu.ru

Блохин Дмитрий Сергеевич, кандидат физико-математических наук, доцент Института физики

Казанский (Приволжский) федеральный университет
ул. Кремлевская, д. 18, г. Казань, 420008, Россия
E-mail: dblohin@kpfu.ru

For citation: Nikitina A.O., Yulmetov A.R., Kusova A.M., Klochkov V.V., Blokhin D.S. Atomistic simulations of PAP248-286 peptide oligomerization. *Uchenye Zapiski Kazanskogo Universiteta. Seriya Estestvennye Nauki*, 2022, vol. 164, no. 2, pp. 185–195. doi: 10.26907/2542-064X.2022.2.185-195.

Для цитирования: Nikitina A.O., Yulmetov A.R., Kusova A.M., Klochkov V.V., Blokhin D.S. Atomistic simulations of PAP248-286 peptide oligomerization // Учен. зап. Казан. ун-та. Сер. Естеств. науки. – 2022. – Т. 164, кн. 2. – С. 185–195. – doi: 10.26907/2542-064X.2022.2.185-195